

Application of Wavelet Transform to Damage Detection in Brittle Materials via Energy and Entropy Evaluation of Acoustic Emission Signals



Juan P. Muszkats, Miguel E. Zitto, Miryam Sassano, and Rosa Piotrkowski

Abstract Acoustic emission (AE) hits from uniaxial compression tests of andesite rock samples were processed with the continuous wavelet transform (CWT). The quest for frequency bands with minimum entropy values arrived at 150 and 250 kHz as those related to macro-fracture mechanisms. A preprocessing algorithm was developed in order to attenuate the influence of reflected signals at the inner interfaces of the material. It is based on the detection of abrupt phase changes of the CWT coefficients. Entropy calculations performed with the hits already processed permitted a reliable study of the AE entropy evolution in the relevant frequency bands and its relationship with the corresponding cumulative AE energy evolution.

1 Introduction

Compressive failure in brittle materials, like rocks submitted to load, consists of an alternation of cracking processes: micro-cracks initiation at certain preexistent flaws followed by micro-cracks coalescence into macro-cracks, macro-cracks growth and branching into new micro-cracks, fragmentation, and final collapse. Thus, tracking of macro-crack initiation and growth seems to be an appealing method for studying

J. P. Muszkats (✉)

Facultad de Ingeniería, Universidad de Buenos Aires, Buenos Aires, Argentina

Universidad Nacional del Noroeste de la Provincia de Buenos Aires, Buenos Aires, Argentina

e-mail: jpmuszkats@comunidad.unnoba.edu.ar

M. E. Zitto

Facultad de Ingeniería, Universidad de Buenos Aires, Buenos Aires, Argentina

M. Sassano

Universidad Nacional de Tres de Febrero, Buenos Aires, Argentina

Facultad de Ingeniería, Universidad de Buenos Aires, Buenos Aires, Argentina

R. Piotrkowski

Escuela de Ciencia y Tecnología, Universidad Nacional de San Martín, Buenos Aires, Argentina

Facultad de Ingeniería, Universidad de Buenos Aires, Buenos Aires, Argentina

© The Author(s), under exclusive license to Springer Nature Switzerland AG 2021

J. P. Muszkats et al. (eds.), *Applications of Wavelet Multiresolution Analysis*,

SEMA SIMAI Springer Series 4, https://doi.org/10.1007/978-3-030-61713-4_5

damage evolution in brittle materials [1–4]. The energy applied (load) to the rocky material is transferred and stored as strain-stress energy in different locations. In those locations where thresholds are suddenly surpassed, energy is dissipated in fracture energy or surface energy. As in any dissipative process, the causes of damage can be described within the frame of the irreversible thermodynamic framework. In this sense, damage parameters, such as entropy generation, account for degradation and loss of structural integrity [5–8].

Acoustic emission (AE) consists of elastic waves generated in the interior of materials. These waves are induced by a rapid change in the stress-strain condition around a given point. In the case of brittle materials, nucleation, advance, opening, and closure of fractures are the main sources for these waves. AE propagates undergoing attenuation and multiple reflections, especially in heterogeneous materials. Eventually, the waves reach the surface, where they can be detected by piezoelectric sensors that transform them into electrical signals, i.e., the AE signals, which are then processed for further analysis. AE signals are hits of very low amplitude (about $10\ \mu\text{V}$) and high frequency (ranging from 1 kHz to 1 MHz), so they have to be immediately amplified. AE equipment stores the waveforms and calculates characteristic parameters such as energy, root mean square (RMS) value, amplitude, rise time, event duration, etc. [9].

AE is ultimately generated by the rupture of atomic bonds. It involves different spatial and temporal scales ranging from microscopic events to seismic faults. Because of this, seismic information and AE in rocks are complementary, both in their applications and in their theoretical basis. Furthermore, AE has been established decades ago as a well-suited tool to evaluate the dynamic state of bulk and surface defects [10]. This can be accomplished by analyzing elastic waves emitted during micro-fracture processes. It is nowadays used in material science and engineering research, including work reported by the authors [2, 3, 11, 12]. Because AE is typically a nonstationary process, wavelet transform (WT) is an appropriate tool for these studies [13].

In previous work [2] the complex Morlet continuous wavelet transform (CWT) was applied to AE signals from dynamic tests conducted on a reinforced concrete slab with a shaking table. The frequency band corresponding to the fracture of concrete was identified by comparing the scale position of maximum CWT values with the response acceleration obtained in seismic simulations. The AE signals were reconstructed in this scale (frequency) band, and cumulative acoustic emission energy (CAE) was calculated. The resulting CAE was compared with the cumulative dissipated energy (CDE) of the tested structure, an accepted parameter for characterizing the mechanical damage in structures: a good agreement was found between the normalized histories of CAE and CDE. Thus, the particular scale (frequency) in which AE signals were reconstructed could be attributed to the fracture of concrete.

In more recent work [14, 15], CWT was applied to AE signals resulting from uniaxial compression tests of andesite rock samples up to breakage. AE signals were filtered into different frequency bands with the CWT. Some of these bands

were identified as characteristic frequencies of the fracture process, in accord with a physical model of seismic focus that describes the advance and propagation of waves during the fracture of brittle materials [4]. Precise results were achieved considering the nonstationary nature of the involved physical processes. The wavelet energy b-value, a variant of the Gutenberg-Richter law that rules in geophysics [3, 16], was successfully applied to trace the inception of dangerous cracks.

In the present paper, which continues [14, 15], we intend to go further into the detection and evaluation of macro-fracture in rocks. To this end entropy and phase studies are introduced in our processing of AE signals.

Irreversible thermodynamic processes cause degradation of materials, and damage is a phenomenon with increasing disorder. The energy dissipated in damage (fracture) results in entropy increase, according to the second law of thermodynamics. Thus, it is important to investigate the damage-entropy relationship while loading material [17]. The premise of Gibbs physical entropy as a limit of the mathematical Shannon entropy is demonstrated in [18] and applied in empirical work in complex systems in other fields [19]. In recent works, Shannon entropy is successfully applied to AE signals for detecting damage in different rocky materials [20, 21]. In the present work, the wavelet Shannon entropy is applied twofold to the same signals as those analyzed in [15]. Firstly, to detect specific signals coming from macro-crack nucleation and advance. Secondly, to follow precisely and concisely the macro-fracturing evolution of andesite rock under load. Another novelty from previous work is that the signals under study were preprocessed with a specifically developed technique. This technique focuses on the phase of complex wavelet coefficients and allowed us to reduce the distortion caused by wave reflections on the detected signals.

2 Experiment

Four cylindrical andesite rock samples were tested as described in [22]. These specimens from Cerro Blanco, San Juan, Argentina, were 75 mm in diameter and 150 mm in length. As illustrated in Fig. 1, the rock samples were subjected to uniaxial compression up to rupture. The equipment consisted of a CGTS machine with a 100 tons capacity of servo-hydraulic type and a closed loop. The actuator displacement speed was 0.12 mm/min.

AE was monitored with three piezoelectric sensors. The present work focuses on the results gathered by the broadband sensor (100–1000 kHz) in one of the samples. The sampling frequency was 1 MHz, the AE system (also shown in Fig. 1) was a PCI-2 two-channel PAC plate, and the commercial software AEWIN was used for the initial determination of classical AE parameters. This experiment resulted in a collection of about 75,000 AE hits, saved in individual files. The analysis of such



Fig. 1 The experimental setup and the AE system

a big quantity of information proved to be time-consuming but manageable for a standard computer.

3 Mathematical Resources

This section contains the description and definition of techniques that we have been consistently using throughout our previous work [14, 15], as well as entropy definitions and the algorithm developed in the present work for preprocessing data.

3.1 Continuous Wavelet Transform

The continuous wavelet transform (CWT) is defined in [23] by means of a continuous wavelet function $\psi(t)$. This function must verify an exponential decay and also that $\int_{\mathbb{R}} \psi = 0$. Given a function $f \in L^2(\mathbb{R})$, its CWT is defined as

$$c(j, k) = \frac{1}{\sqrt{|j|}} \int_{-\infty}^{\infty} f(t) \overline{\psi\left(\frac{t-k}{j}\right)} dt \quad (1)$$

if $j \neq 0$, while $c(0, k) = 0$. In each CWT coefficient $c(j, k)$, the value of j indicates a scale (and therefore a frequency), while k denotes time displacement.

In the present work, we used the Morlet wavelet defined by

$$\psi(t) = \pi^{-\frac{1}{4}} \cdot e^{6it} \cdot e^{-\frac{t^2}{2}} \quad (2)$$

Being continuously defined for every j and k , practical implementation arises numerical issues. Approximation algorithms and details can be found in [24].

In order to illustrate the CWT when applied to AE, the plot of a typical hit is shown in the upper part of Fig. 2. Its corresponding scalogram in the lower part of Fig. 2 illustrates the distribution in time and frequency of the wavelet energy density $|c(j, k)|^2$, with value increasing from darker to lighter tones.

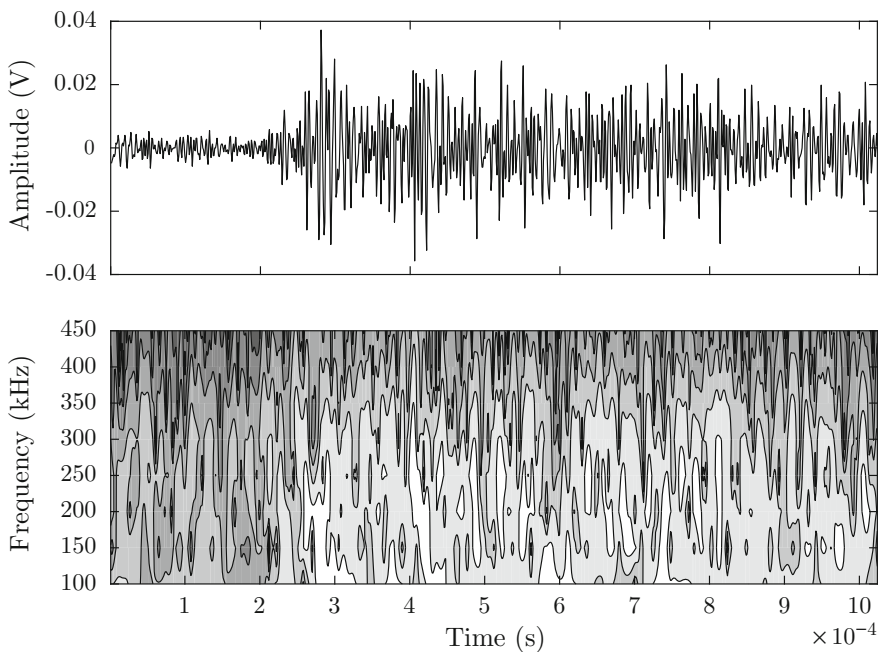


Fig. 2 A typical hit. Upper: waveform. Lower: scalogram (increasing from darker to lighter tones)

The simplest way to perform bandpass filtering with the CWT consists in reconstructing the signal only with the CWT coefficients of the desired frequencies. Figure 3 illustrates this procedure applied to the same previous hit, filtered at 250 kHz. The bandpass frequency is clear in the corresponding scalogram, shown in Fig. 3.

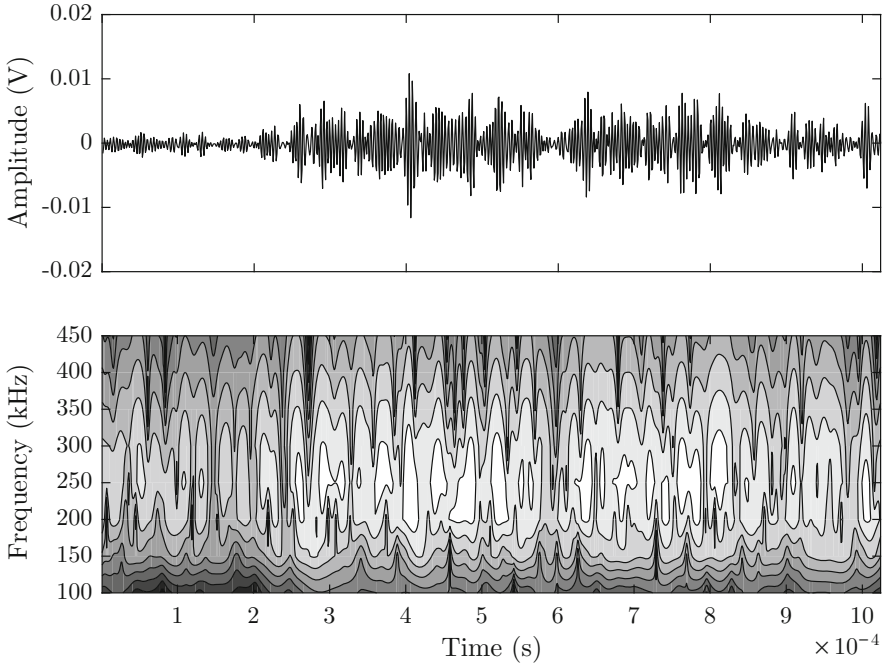


Fig. 3 Same hit as in Fig. 2 filtered around 250 kHz. Upper: waveform. Lower: scalogram (increasing from darker to lighter tones)

The acoustic emission energy (AEE) of a hit is defined in [3] as

$$AEE = \sum x_i^2 \Delta t \quad (3)$$

where x is the reconstructed signal after filtering and Δt is the sample rate.

3.2 Wavelet Entropy

The Shannon entropy can be adapted as in [11] to obtain a measure of the intrinsic order in a signal by means of its CWT coefficients. When CWT is numerically implemented, only a finite quantity of the c_{jk} coefficients defined by (1) can be obtained. Thus, the wavelet power (WP) corresponding to the j th scale is defined by

$$WP_j = \sum_{k=1}^N |c_{jk}|^2 \quad (4)$$

The fraction of wavelet power corresponding to time k is expressed by the p_{jk} coefficients:

$$p_{jk} = \frac{|c_{jk}|^2}{WP_j} \quad (5)$$

With these elements, wavelet entropy of the j th band is formally equal to the Shannon entropy:

$$S_j = - \sum_{k=1}^N p_{jk} \log p_{jk} \quad (6)$$

Figure 4 shows for the hit previously considered the values of entropy calculated for the different scales (frequencies). Coalescence of micro-cracks into macro-cracks, which implies the transition from less to more organized structures, is expected to express in frequencies with lower entropy. Therefore, those frequencies for which relative minima of entropy occur are of special interest.

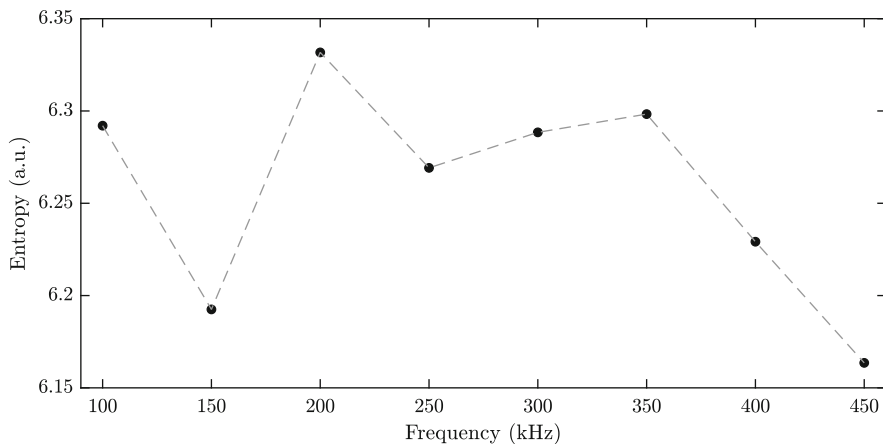


Fig. 4 The same hit as in Fig. 2 reaches relative minima of entropy for the 150 and 250 kHz bands

3.3 Preprocessing

Each detected AE hit is the complex consequence of a large number of random events [25]. In particular, reflections at the multiple interfaces present in natural rocks constitute a special problem. If a second mechanical pulse reaches the detector while the first one is still operating, the apparent duration, the waveform, and the entropy of this composite signal are affected. To reduce the effect of reflections,

a special algorithm was developed. Given that the Morlet wavelet coefficients are complex numbers, it is expected to find their phase varying cyclically when analyzing a perfectly periodic signal. When reflections occur, they imply the sudden overlapping of vibrations, with the consequent phase changes. These phase variations are detected by studying the deviations from the expected cyclical plot. Figure 5 shows, for the same hit previously studied, the phase plot of the CWT coefficients corresponding to the 250 kHz scale. The square denotes the instant when the amplitude surpasses a threshold for the first time. Diamonds mark the instants when sudden phase changes occur. Those diamonds closest to the square delimit the relevant part of the hit, preserved for ulterior entropy calculations.

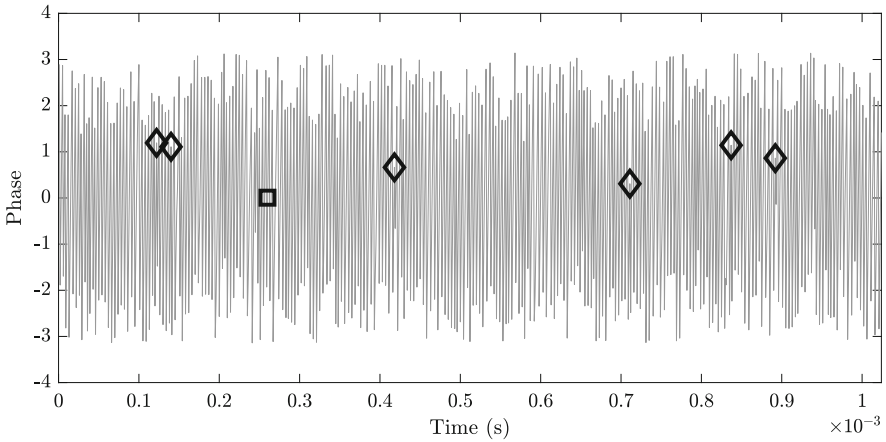


Fig. 5 Same hit as in Fig. 2 filtered around 250 kHz: phase of wavelet coefficients versus time. Square: amplitude surpasses a threshold for the first time. Diamonds: sudden phase change

Thus, the most relevant (and least distorted) part of each hit is selected, and this analysis is performed separately for each scale (see Fig. 6). For our present work, it was only after the described preprocessing that entropy for every hit and scale was calculated.

4 Results and Discussion

Despite being continuously defined in (1), the CWT can only be calculated for a discrete set of values j and k . Moreover, the Heisenberg uncertainty principle imposes an unavoidable trade-off between time and frequency localization. Therefore, the choice of the scales for which the CWT is calculated must rely upon a trustworthy frequency resolution. In the present work, several features were taken into account: the range of the broadband sensor (100–1000 kHz), the sampling frequency (1 MHz), and the duration of the shortest hits (estimated to be

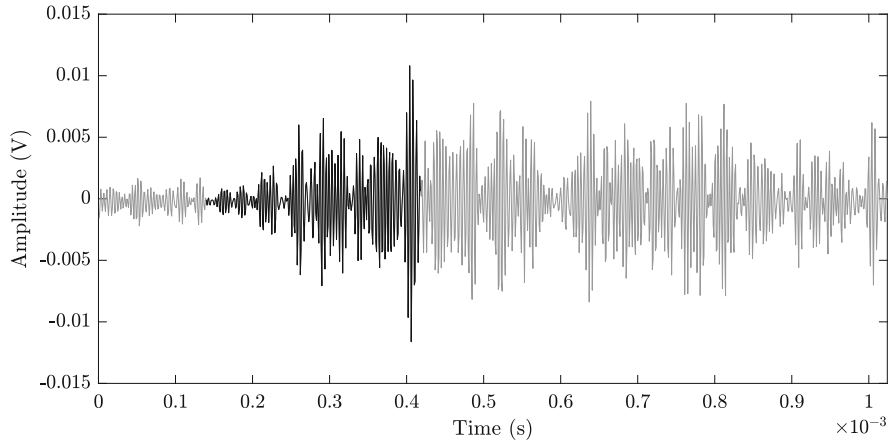


Fig. 6 Preprocessed hit. Lighter plot: original filtered hit. Darker plot: preserved section of the hit

about $10\ \mu\text{s}$). Under these premises, the width of frequency bands was chosen to be 50 kHz. Figures 2 and 3 illustrate this choice.

In previous work [14, 15] the detection of characteristic frequencies relied upon energy considerations. Frequency bands near 150 and 250 kHz were chosen to be those most representative of the fracture mechanism. Figure 7 plots the cumulative AEE calculated according to (3). The signal with its whole frequency content is plotted as a dashed line, while the signal reconstructed at 150 kHz is plotted in black, and the signal reconstructed at 250 kHz is plotted in gray. Both filtered signals and the original signal show similar energy evolution and jumps. The 150 and the 250 kHz reconstructed signals also show a very similar energy level throughout the whole experiment.

The entropy concept provides a complementary tool that proved to be consistent with previous results. For the present purposes, entropy is considered as a measure of disorder in a signal. Therefore, lower entropy values suggest the occurrence of more organized phenomena. After the preprocessing already described, every single hit was analyzed as in Fig. 4. Frequencies with relative minimum entropy were detected according to a threshold criterion (eventually, a single hit might have several relative minima).

Figure 8 is a histogram which accounts for the density of hits that present a minimum entropy at a given frequency band. Table 1 gathers basic statistical information about entropy and frequency after analyzing the whole set of hits. It also shows the average time duration of the preprocessed hits, discriminated by frequency band. This duration showed to be consistently smaller as frequency increases.

According to Table 1, 150 and 250 kHz frequencies turned out to be those for which entropy reaches a relative minimum more often. It is also important to notice

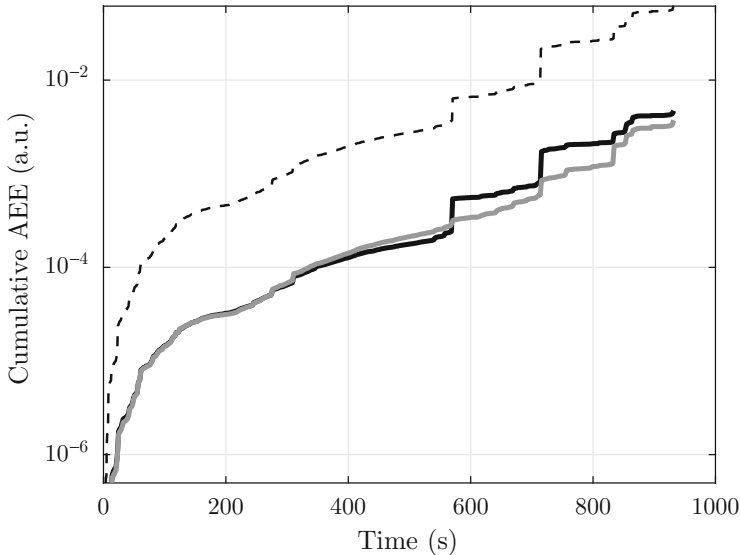


Fig. 7 Cumulative AEE along the test. Dashed: whole frequency content. Black: 150 kHz. Gray: 250 kHz

Table 1 Preprocessed hits statistics

Frequency (kHz)	Number of entropy minima	μ (entropy mean value)	σ (entropy standard deviation)	Average time duration (milliseconds)
100	891	5.7	0.5	0.65
150	26847	4.9	0.7	0.37
200	16612	4.8	0.8	0.37
250	20988	4.6	0.8	0.29
300	9795	4.5	0.8	0.25
350	9291	3.7	1	0.12

that these minima were mostly reached by the end of the experiment, as shown in Fig. 8. Therefore, these hits are of special interest and most likely to express a characteristic frequency of the fracturing process. Figure 9 shows the entropy and its time evolution for those hits which attain a minimum at 150 kHz (black line) and those which attain a minimum at 250 kHz (gray line). In order to make it easier to read the plot, a moving mean of 1000 points was applied to the results. The entropy value for the 250 kHz proved to be consistently smaller throughout the whole experiment. This would imply that the 250 kHz frequency band is more strongly related to the advance of macro-cracks, a more organized phenomenon.

The AEE defined in (3) can be calculated for reconstructed hits after bandpass filtering. It is of particular interest to trace the time evolution of this energy: therefore the cumulative AEE for each frequency band was calculated. Upper

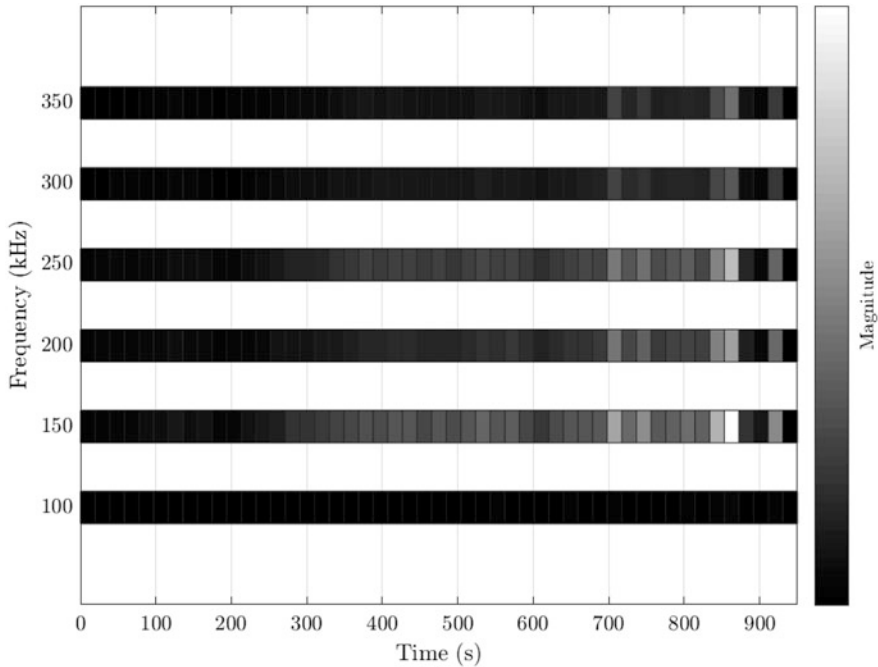


Fig. 8 Frequency bands and density of hits with minimum entropy

Fig. 10 shows the cumulative AEE for the 150 kHz band, while lower Fig. 10 shows the cumulative AEE for the 250 kHz band (both in thin lines). These graphs also show the time evolution of the corresponding entropy already shown in Fig. 9. It can be appreciated that entropy evolution changes significantly, even shows relative minima, before cumulative energy jumps. That is, it anticipates the expression of dangerous damage.

Fracture in rocks is an interplay of macro-fracture, nucleation, advance and branching into micro-cracks, followed by further coalescence of micro-cracks into macro-cracks. The results displayed in Figs. 7, 8, 9, and 10 suggest that the main features of the whole fracturing process in andesite can be followed by the evolution of wavelet energy and wavelet entropy in the selected bands. Moreover, the 250 kHz band, due to its lower entropy values, seems to be connected to nucleation and advancement of macro-cracks.

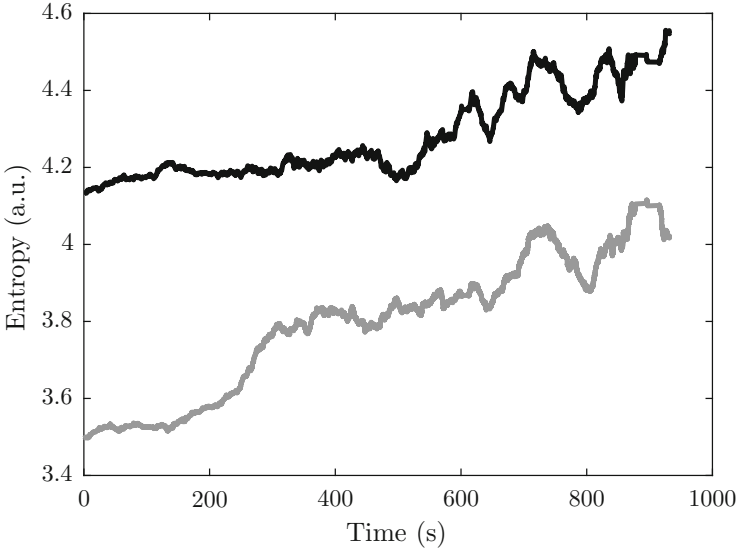


Fig. 9 Entropy of preprocessed hits at 150 kHz (black) and 250 kHz (gray). A moving mean of 1000 points was applied

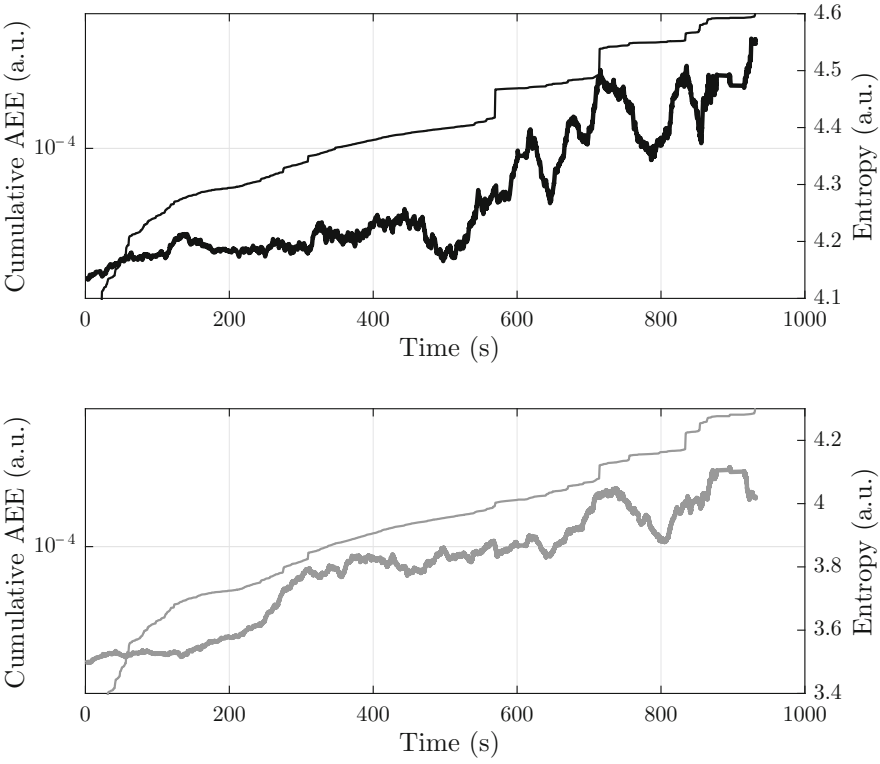


Fig. 10 AEE (thin) and entropy (thick). Upper: at 150 kHz. Lower: at 250 kHz

5 Conclusions

The minimum entropy criterion applied to AE hits resulted in a reliable tool for the detection of relevant frequency bands. It is sensibly improved by the preprocessing of the signals, which reduces the distorting effects due to inner reflections in the studied material.

Comparison with previous work and other criteria [14, 15] reinforces the conclusion that the 150 and 250 kHz are characteristic frequencies of the andesite rock, related to macro-fracture mechanisms.

Those hits most related to each of these bands were specifically studied. Their entropy evolved in accordance with the cumulative AEE. Major changes in AEE are anticipated and accompanied by abrupt oscillations in entropy. These sudden changes, both in AEE and entropy, indicate an abrupt reorganization of the material rheological state.

Acknowledgments The present work received financial support and is part of the Program UBACyT 20020160100038BA.

References

1. Huq, F., Liu, J., Tonge, A.L., Graham-Brady, L.: A micromechanics based model to predict micro-crack coalescence in brittle materials under dynamic compression. *Eng. Fract. Mech.* (2019). <https://doi.org/10.1016/J.ENGFRACMECH.2019.106515>
2. Zitto, M.E., Piotrkowski, R., Gallego, A., Sagasta, F., Benavent-Climent, A.: Damage assessed by wavelet scale bands and b-value in dynamical tests of a reinforced concrete slab monitored with acoustic emission. *Mech. Syst. Signal Process.* (2015). <https://doi.org/10.1016/J.YMSSP.2015.02.006>
3. Sagasta, F., Zitto, M.E., Piotrkowski, R., Benavent-Climent, A., Suarez, E., Gallego, A.: Acoustic emission energy b-value for local damage evaluation in reinforced concrete structures subjected to seismic loadings. *Mech. Syst. Signal Process.* (2018). <https://doi.org/10.1016/j.ymssp.2017.09.022>
4. Filipussi, D., Piotrkowski, R., Ruzzante, J.: Characterization of a crack by the acoustic emission signal generated during propagation. *Procedia Mater. Sci.* (2012). <https://doi.org/10.1016/j.mspro.2012.06.036>
5. Amiri, M., Modarres, M.: An entropy-based damage characterization. *Entropy* (2014). <https://doi.org/10.3390/e16126434>
6. Imanian, A., Modarres, M.: A thermodynamic entropy-based damage assessment with applications to prognostics and health management. *Struct. Health Monit.* (2018). <https://doi.org/10.1177/1475921716689561>
7. Vaughn, N., Kononov, A., Moore, B., Rougier, E., Viswanathan, H., Hunter, A.: Statistically informed upscaling of damage evolution in brittle materials. *Theor. Appl. Fract. Mech.* (2019). <https://doi.org/10.1016/J.TAFMEC.2019.04.012>
8. Kang, Y., Liu, H., Aziz M., Kassim, K.A.: A wavelet transform method for studying the energy distribution characteristics of microseismicities associated rock failure. *J. Traffic Transp. Eng. (Engl. Ed.)* (2019). <https://doi.org/10.1016/J.JTTE.2018.03.007>

9. Grosse, C., Ohtsu, M. (eds.): *Acoustic Emission Testing*. Springer, Heidelberg (2008)
10. Ono, K. : *Acoustic Emission*. In: Rossing T.D. (ed.) *Springer Handbook of Acoustics*. Springer Handbooks. Springer, New York (2014)
11. Piotrkowski, R., Castro, E., Gallego, A.: Wavelet power, entropy and bispectrum applied to AE signals for damage identification and evaluation of corroded galvanized steel. *Mech. Syst. Signal Process.* (2009). <https://doi.org/10.1016/j.ymssp.2008.05.006>
12. Piotrkowski, R., Gallego, A., Castro, E., García-Hernandez, M.T., Ruzzante, J.E.: Ti and Cr nitride coating/steel adherence assessed by acoustic emission wavelet analysis. *NDT & E Int.* (2005). <https://doi.org/10.1016/J.NDTEINT.2004.09.002>
13. Meyer, Y., Ryan, R.: *Wavelets: algorithms & applications*. Society for Industrial and Applied Mathematics, Philadelphia (1993)
14. Filipussi, D., Muszkats, J., Sassano, M., Zitto, M., Piotrkowski, R.: Fractura de roca andesita y análisis espectral de señales de emisión acústica. *Tecnura*. **23**(61), 45–56 (2019)
15. Muszkats, J.P., Filipussi, D., Zitto, M.E., Sassano, M., Piotrkowski, R.: Detection of fracture regimes in andesite rock via the energy evolution of acoustic emission signals in relevant frequency bands. In: Ceballos, L., Gariboldi, C., Rocca, B. (eds.) *VII Congreso de Matemática Aplicada, Computacional e Industrial*, pp. 489–492. ASAMACI, Río Cuarto, Córdoba (2019)
16. Rao, M.V.M.S., Prasanna Lakshmi, K.J.: Analysis of b-value and improved b-value of acoustic emissions accompanying rock fracture. *Curr. Sci.* (2005). <https://doi.org/10.2307/24110936>
17. Mahmoudi, A., Mohammadi, B.: On the evaluation of damage-entropy model in cross-ply laminated composites. *Eng. Fract. Mech.* (2019). <https://doi.org/10.1016/J.ENGFRACMECH.2019.106626>
18. Truffet, L.: Shannon entropy reinterpreted. *Rep. Math. Phys.* (2017). [https://doi.org/10.1016/S0034-4877\(18\)30050-8](https://doi.org/10.1016/S0034-4877(18)30050-8)
19. Dobovišek, A., Markovič, R., Brumen, M., Fajmut, A.: The maximum entropy production and maximum Shannon information entropy in enzyme kinetics. *Phys. A Stat. Mech. Appl.* (2018). <https://doi.org/10.1016/J.PHYSA.2017.12.111>
20. Chai, M., Zhang, Z. Duan, Q.: A new qualitative acoustic emission parameter based on Shannon's entropy for damage monitoring. *Mech. Syst. Signal Process.* (2018). <https://doi.org/10.1016/J.YMSSP.2017.08.007>
21. Bressan, G., Barnaba, C., Gentili, S., Rossi, G.: Information entropy of earthquake populations in northeastern Italy and western Slovenia. *Phys. Earth Planet. Inter.* (2000). <https://doi.org/10.1016/J.PEPI.2017.08.001>
22. Filipussi, D.A., Guzmán, C.A., Xargay, H.D., Hucaíluk, C., Torres, D.N.: Study of acoustic emission in a compression test of andesite rock. *Procedia Mater. Sci.* (2015). <https://doi.org/10.1016/J.MSPRO.2015.04.037>
23. Boggess, A., Narcowich, F.J.: *A First Course in Wavelets with Fourier Analysis*, 2nd edn. Wiley, Hoboken (2009)
24. Torrence C., Compo G.P.: A practical guide to wavelet analysis. *Bull. Am. Meteorol. Soc.* (1998). [https://doi.org/10.1175/1520-0477\(1998\)079<0061:APGTWA>2.0.CO;2](https://doi.org/10.1175/1520-0477(1998)079<0061:APGTWA>2.0.CO;2)
25. López Pumarega, M.I., Armeite, M., Ruzzante, J.E., Piotrkowski, R.: Relation between amplitude and duration of acoustic emission signals. *Rev. Quant. Nondestruct. Eval.* **22**, 1431–1438 (2003)